ISSN 1330–0008
CODEN FIZAE4

EFFECT OF TEMPERATURE AND INDIUM ADDITION ON THE WORK HARDENING CHARACTERISTICS OF Al–0.21wt%Au ALLOY

F. ABD EL-SALAM, A. M. ABD EL-KHALEK and R. H. NADA

Physics Department, Faculty of Education, Ain Shams University, Cairo, Egypt

Received 27 November 2000; revised manuscript received 23 April 2001
Accepted 25 June 2001

Tensile characteristics of both Al–0.21wt%Au and Al–0.21wt%Au–0.21wt%In alloys were investigated in the temperature range 493 K to 553 K. The coefficient of work hardening, $\chi = \partial\sigma^2/\partial\epsilon$, yield stress, σ_y, and fracture stress, σ_f, decreased with increasing deformation temperature (T) and exhibited abrupt increase at about 523 K. On the other hand, the fracture strain, ϵ_f, and dislocation slip distance, L, increased with increasing deformation temperature and exhibited minima at about 523 K. The activation energy was determined in the range around 523 K to clarify the observed change in the behaviour of the hardening characteristics of the investigated samples.

PACS numbers: 62.20.-x, 83.50.Nj UDC 531.4–522, 531.431.42

Keywords: stress-strain, deformation temperature, dislocations, hardening characteristics, softening, incoherent precipitates

1. Introduction

Many authors (e.g. see Refs. [1–3]) have investigated the effect of trace elements and temperature on mechanical characteristics of various binary and ternary alloys. A detailed investigation [4] on the structure and morphology of precipitates in Al–Au alloys showed that the solubility of Au in Al is approximately 0.3wt% at 640 °C, and decreased with decreasing temperature. Also, a small amount of Au alloyed to Al is sufficient to produce a considerable precipitation hardening on aging at temperatures ranging from 100 °C to 200 °C. Hardening with aging was mainly attributed [4] to the homogeneous distribution of the existing plate-like precipitates and their small size. It was found [5,6] that aging of Al–0.21wt%Au alloys at low temperatures (200 °C) up to 20 hours, produced platelets of Al_2Au precipitates with coherent nature. Also, it was reported [5] that prolonged aging

treatments at elevated temperatures for Al–Au alloys in the bulk state produce large coherent precipitates. By analyzing the precipitation sequence in the Al–Au system by transmission electron microscopy and X-ray techniques [4], it was suggested that the formation of the plate-like metastable precipitates, η', which form mainly on the (100) matrix planes at certain aging conditions, precede the formation of the equilibrium phase $\eta(Al_2Au)$.

The present work aims at studying the effect of both tensile deformation at different temperatures and indium addition on the work hardening and structure characteristics, through stress-strain tests and X-ray measurements, for the Al–0.21wt%Au alloy.

2. Experimental procedure

High purity Al, Au and In (99.999) were used to prepare the alloys Al–0.21wt%Au (alloy A) and Al–0.21wt%Au–0.21wt%In (alloy B). The components were weighted and melted in a graphite crucible in air under chloride flux to prevent oxidation. Casting was carried out in graphite moulds. The rod-shaped ingots were drawn to wires of diameter 0.4 mm after homogenization for 3 days at 823 K. From each alloy, two groups of samples were annealed for 4 h at 793 K. The first group of samples of each alloy was slowly-cooled to room temperature (RT $\approx$ 300 K) at a cooling rate of 2 K/min to obtain the complete precipitation. The second group of samples was rapidly quenched from 793 K to RT to obtain samples containing the supersaturated solid solutions. The average grain diameter was determined with an optical metallurgical microscope and applying the linear intercept method where about thirty grains were considered.

The stress-strain relations were carried out with a strain rate of 4×10^{-4} s^{-1} for the four groups of samples by using a conventional tensile testing machine in the temperature range from 493 K to 553 K in steps of 10 K. The elongation was measured by a dial gauge with sensitivity of 10^{-2} mm. The yield stress, σ_y, considered as the stress corresponding to the first significant deviation from linearity in the starting part of the stress–strain curves or the macroscopic elastic limit [7], and the fracture stress, σ_f, which is taken as the last maximum stress applied to the sample before fracture, were determined from the stress–strain curves (see Fig. 1).

The microstructure of the test samples was examined using a Philips X-ray diffractometer (PW 1050/70), CuKα radiation of wavelength 0.1542 nm.

3. Results

Stress-strain curves for slowly-cooled and quenched samples of alloy A at different deformation temperatures are shown in Fig. 1. The temperature dependence of the yield stress, σ_y, the fracture stress, σ_f, and the fracture strain, ϵ_f, are shown in Figs. 2a, b and c. A decreasing behaviour of σ_y and σ_f was observed with in-

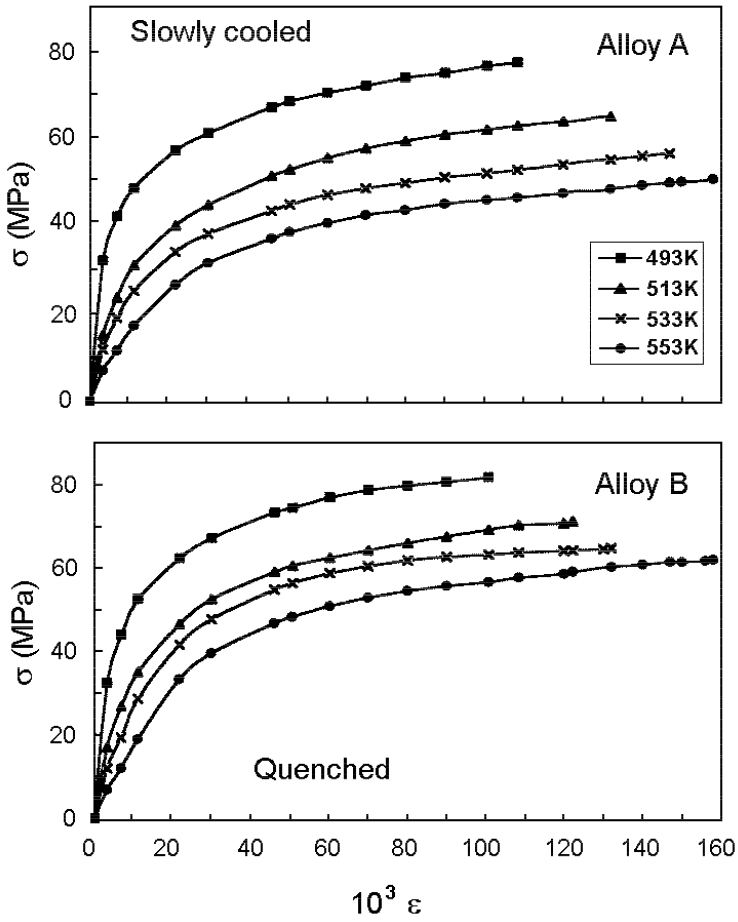

Fig. 1. Stress–strain curves for slowly-cooled and quenched samples of alloy A *(*Al–*0.21wt%*Au*) at different deformation temperatures.*

creasing deformation temperature interrupted with a sudden increase at about 523 K, followed by a continuous decrease for each of these parameters above 523 K. On the other hand, ϵ_f showed a reverse behaviour of increasing at higher deformation temperatures and showed a sudden decrease at 523 K, followed by a continuous increase afterwards.

From Fig. 2, it is clear that the values of σ_y and σ_f are generally lower for the slowly-cooled samples than those of the quenched samples. Also, these values are lower for the indium-free samples (alloy A) than those of the ternary-alloy samples (alloy B). The work hardening coefficient, χ, predicted by Mott's model [8,9] is given by

$$\chi = \frac{\partial \sigma^2}{\partial \epsilon} = \frac{G^2 b}{2\pi^2 L}\,, \tag{1}$$

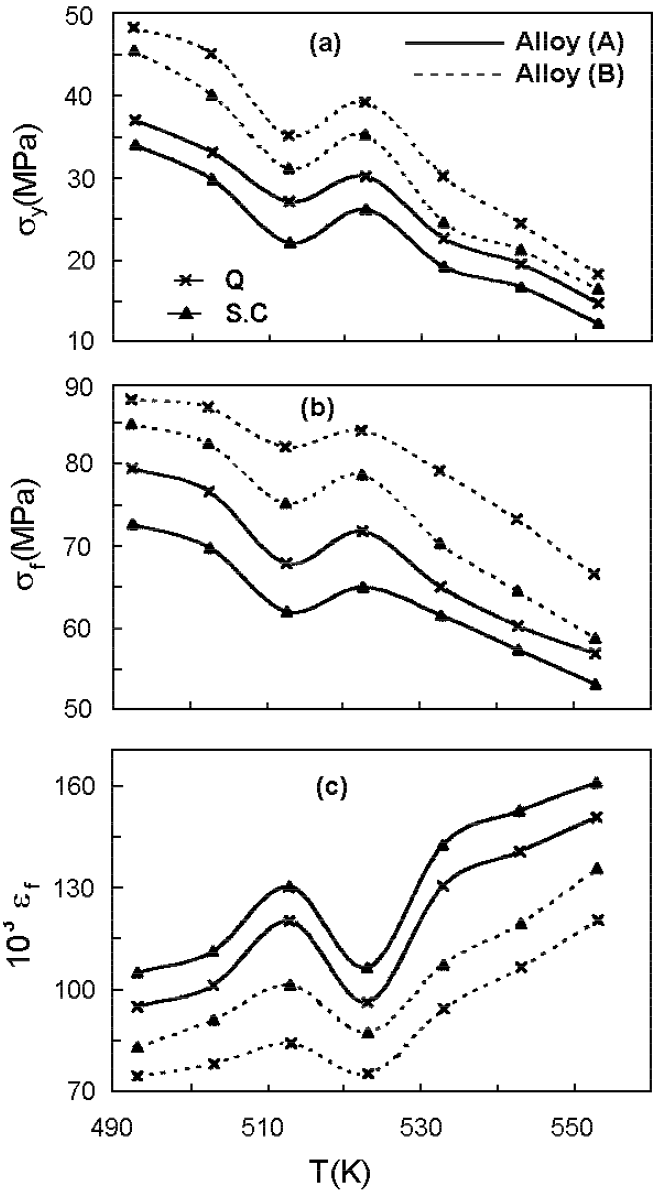

Fig. 2. The temperature dependence of σ_y, σ_f and ϵ_f for slowly-cooled and quenched samples for alloys A *and* B.

where G is the shear modulus of the material ($G = 2.7 \times 10^{10}$ N/m^2), b is the Burger's vector ($b = 2.86 \times 10^{-10}$ m) and L is the average distance slipped by dislocations in their motion.

The $\sigma^2 - \epsilon$ relations for all tested samples showed straight lines. The slope of each line gives the coefficient of work hardening, χ. Using Eq. (1), the corresponding dislocation slip distance L was calculated.

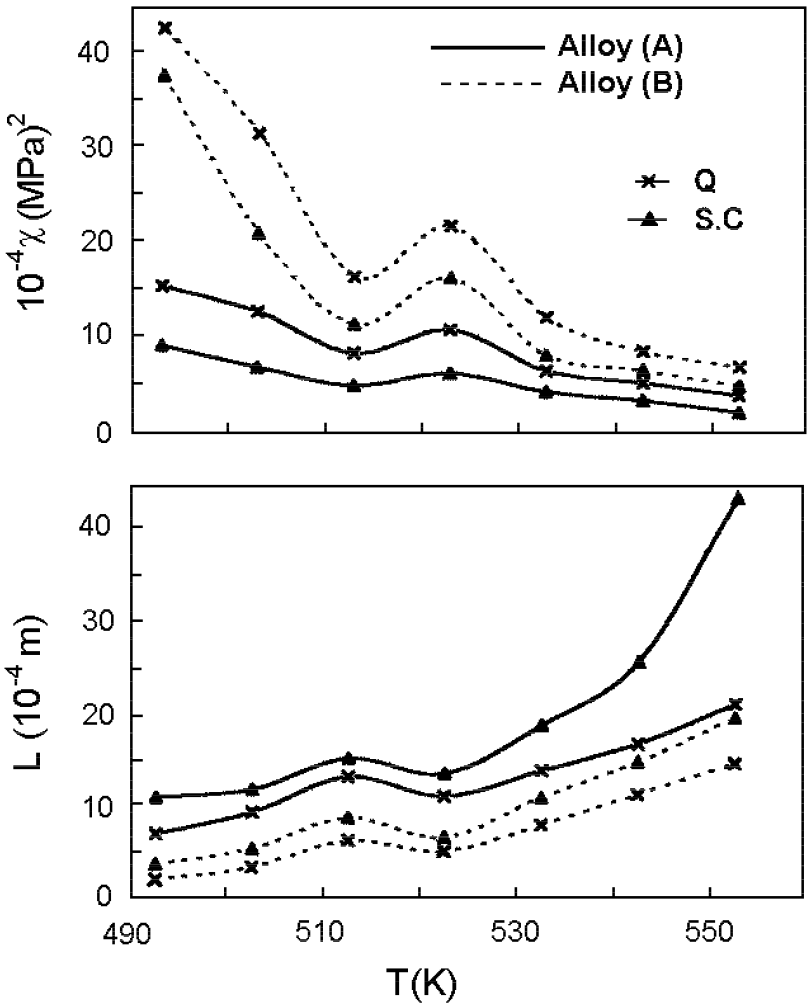

Fig. 3. Temperature dependence of the coefficient of work hardening, χ, and dislocation slip distance, L, for the tested samples.

Figure 3 shows the temperature dependence of the work hardening coefficient, χ, and the corresponding slip distance L for the tested samples.

The functional form of the curved part of the stress–strain curve after yielding can be clarified through the stress dependence of the coefficient of work hardening, χ, and the strain-hardening behaviour.

Representative curves relating χ or L and σ for slowly-cooled indium free samples (alloy A) at different deformation temperatures are shown in Figs. 4a and b, respectively. The observed decrease of χ following its initial increase, observed clearly at 493 and 513 K for small σ, and the increase of L when increasing the applied stress indicate the dominance of a softening behaviour.

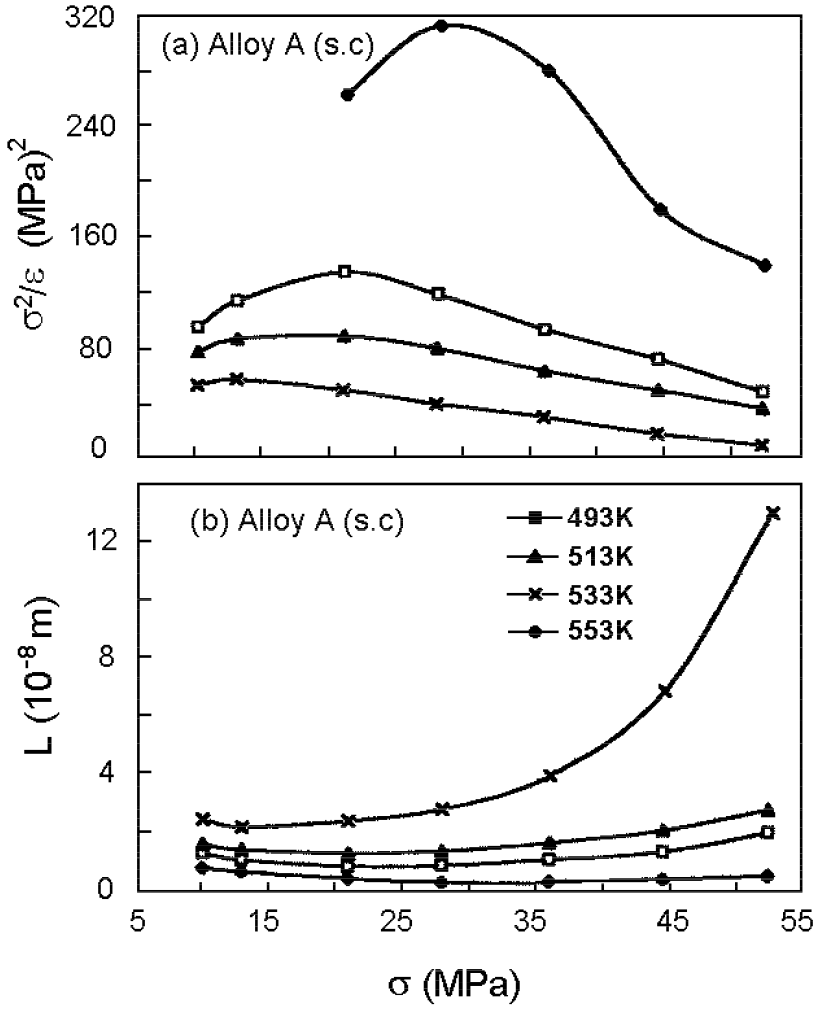

Fig. 4. The stress dependence of: (a) the work hardening coefficient, χ, and (b) the corresponding dislocation slip distance, L, at different deformation temperatures, for the slowly-cooled samples of alloy A.

Figures 4a and b show that the critical stress, σ_c, characterizing the start of the softening behaviour, depends on the deformation temperature and the inter-

nal structure of the sample. The role of the stress and temperature is clear from Fig. 4 where the critical stress σ_c, at which the parabolic part of the stress–strain curve starts, decreased with increasing the deformation temperature for all tested samples.

The strain hardening behaviour of the tested samples is described by applying the Hollomon equation [10],

$$\sigma_t = A\epsilon_t^m \,, \tag{2}$$

where σ_t is the true stress, ϵ_t is the true strain, A is the strain hardening coefficient and m is the strain hardening exponent (or the strain hardening rate).

The $\log \sigma_t$ versus $\log \epsilon_t$ relation for all tested samples at different deformation temperatures gave two straight lines, thus showing a "double–m" strain hardening behaviour [11]. This indicates that the tested samples undergo a marked change in the strain hardening rate during the tensile testing at a certain critical stress, σ_c, and points to the start of the softening behaviour. Assuming that the strain-hardening rate at the critical strain, ϵ_c, can be expressed by [11]

$$m_1 - m_2 = \frac{\log(A_2/A_1)}{\log \epsilon_c} \,, \tag{3}$$

or,

$$\frac{m_1}{m_2} = \frac{\log(\sigma_c/A_1)}{\log(\sigma_c/A_2)} \,, \tag{4}$$

the temperature dependence of σ_c values for both alloys is given in Fig. 5a.

The energies controlling the change of the hardening behaviour of the tested samples, considered to obey an Arrhenius-type relation, can be obtained from the slopes of straight lines relating $\ln \sigma_c$ and $1000/T$, as shown in Fig. 5b. The two separate stages of Fig. 5b correspond to the two stages of the strain hardening behaviour. Table 1 shows the calculated activation energy values.

Table 1. Values of the activation energies for quenched (Q) and slowly-cooled (SC) samples.

Alloy A	Act. energ.	
Cooling	Stage II	Stage I
Q	0.9 eV	0.82 eV
SC	0.9 eV	0.82 eV

Alloy B	Act. energ.	
Cooling	Stage II	Stage I
Q	1.2eV	0.91 eV
SC	1.2eV	0.91 eV

In Fig. 5b, the nearly parallel straight lines at any of the two stages show that the observed sudden softening, which might be due to twinning, occurred independently of the initial state of the tested sample, but depends on the temperature range used and the indium addition.

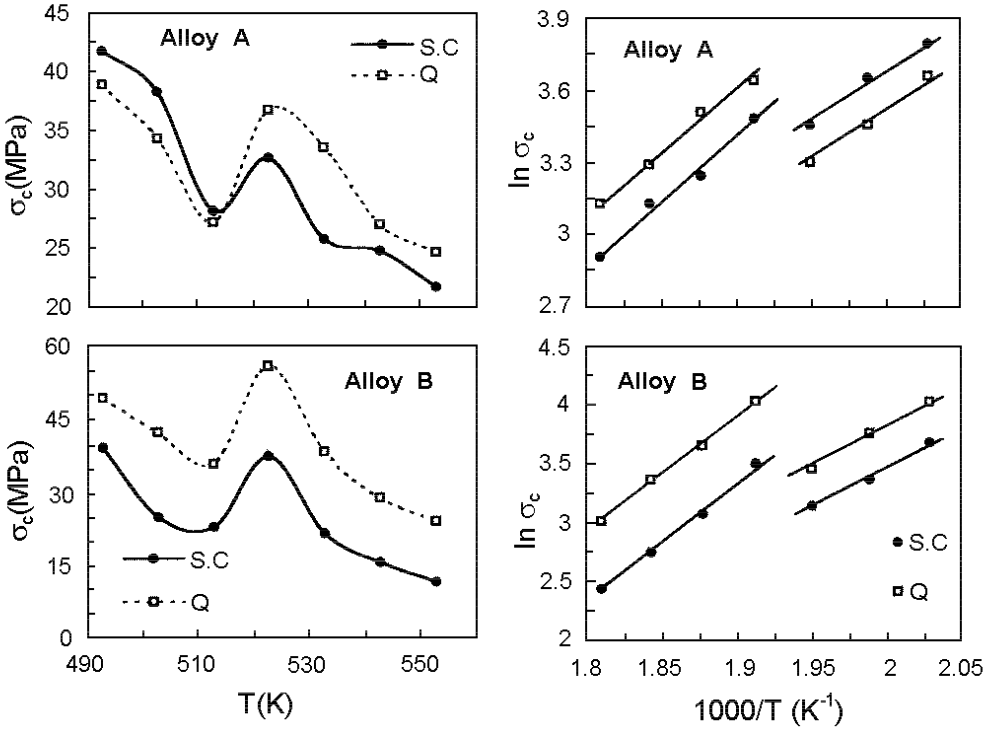

Fig. 5. (left) Temperature dependence of σ_c for the tested samples. (right) $\ln \sigma_c$ *versus* $1000/T$ *relation for the tested samples.*

The microstructure was investigated for the quenched and slowly-cooled deformed samples of both alloys. The full width at half maximum intensity, $\Delta 2\Theta$, and the integral intensity, I, increased with increasing deformation temperature and both parameters exhibited maxima at 523 K for all tested samples. The lattice parameter, a, of Al matrix changed with deformation temperature and exhibited a minimum at 523 K. These observations are shown in Fig. 6 for the slowly-cooled samples of both alloys as representative example.

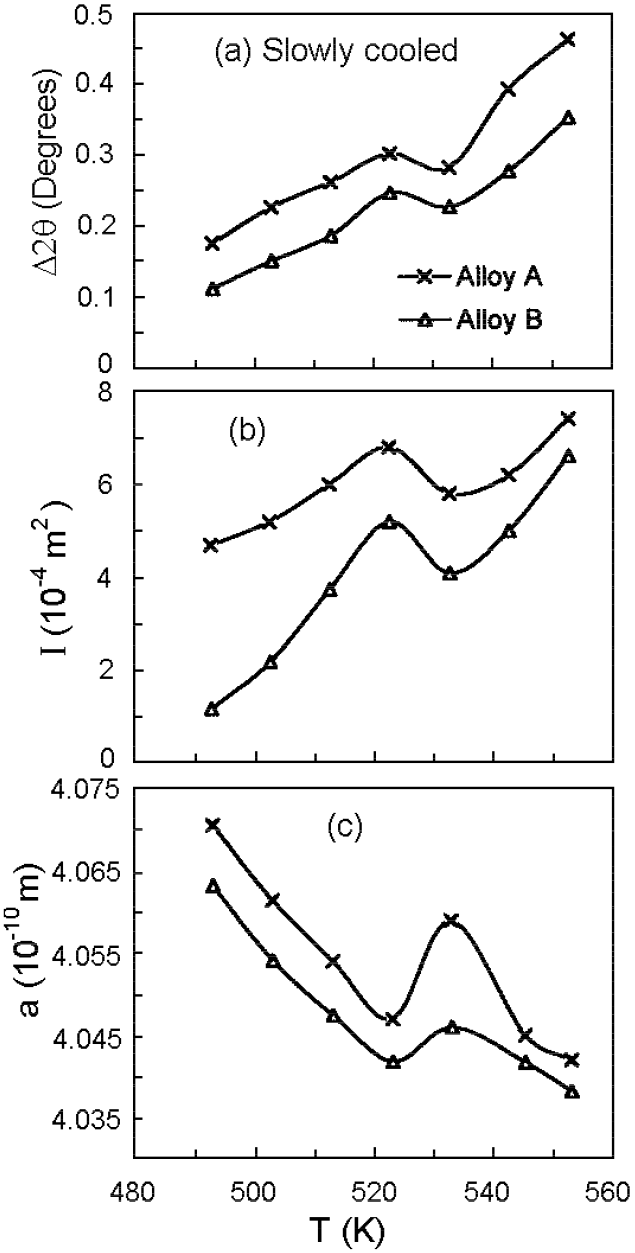

Fig. 6. The temperature dependence of: (a) X*-ray full-width-at-half-maximum intensity,* $(\Delta 2\Theta)$*, (b) Integral intensity,* I*, and (c) lattice parameter,* a*, for the slowly-cooled samples.*

4. Discussion

The change of the stress–strain levels in Fig. 1 and the anomalous ordering observed at about 523 K can be attributed mainly to dynamical precipitation hardening. Despite the small amount [12] of Au (0.21wt%) alloyed to Al, the observed hardening might be due to the formation of the small sized plate-like coherent η precipitates Al_2Au, most of which lose coherency above 523 K during the stages of growth [13]. This is supported by the X-rays diffraction patterns obtained for the as-quenched and from slowly-cooled samples of both alloys and the patterns obtained for these samples after deformation at different working temperatures.

The external factors and the internal state of a tested sample are expected to modify largely the internal effective forces that impart the material its characteristic mechanical properties such as strength, ductility and toughness [14].

For slowly-cooled samples, the saturated solid solution decomposes on cooling by preferential precipitation on grain boundaries [15]. The cell boundaries move discontinuously forming the equilibrium α(Al), and the plate-like η precipitate, (Al_2Au) phases [12]. The vacancies and other lattice concentration of defects are, therefore, low for slowly-cooled samples compared with that of the quenched samples. At low deformation temperatures, thermal activation is minimal and defect creation is naturally difficult and less probable. Accordingly, larger capacity of the matrix to accept excess amounts of defects is observed as is clear from the observed higher elastic limits (higher values of σ_y) and the higher values of the hardening parameters σ_y, σ_f (Figs. 2a and b) and χ (Fig. 3) obtained at lower working temperatures, below 523 K. The peaks of these parameters observed at about 523 K correspond to a large amount of age hardening attained due to the homogeneous distribution of the many plate-like η precipitates and their small size, which keeps them coherent with the matrix. Besides this homogeneous distribution, matrix dislocations also contribute to this hardening as they act as heterogeneous sites for nucleation of precipitate plates [1].

The relative increase of the strength level of the quenched samples in comparison to that of the slowly-cooled samples implied that the solute Au–vacancy pairs, in the quenched samples, migrated to dislocations. The dispersion of solute (Au) atoms on the slip planes presents some frictional forces on the motion of dislocations. This causes a retardation effect on the mobile lattice defects [16]. The slower the quench, the greater is the possible vacancy migration distance to the grain boundary sink and the less will be the density of retained vacancies. This will affect precipitate formation since no precipitates can be formed in a vacancy-free region.

At 523 K, thermally induced growth of η precipitate particles attains a maximum. As the dissolution of small particles is faster than that for large particles, concentration gradients will exist in the matrix. Solute atoms will diffuse away from the vicinity of small particles towards regions in the vicinity of large particles where they are precipitated. The existing matrix dislocations act, therefore, as heterogeneous sites for nucleation of precipitate plates with the result of the observed increase in strength (Figs. 2a and 3).

Above 523 K, during the growth of the η precipitate particles and due to the

high value of mismatch parallel to the broad faces of η precipitate ($\approx 4.8\%$), the loss of coherency [1,14] at these interfaces usually takes place during the very early stages of growth [13] of the incoherent stable precipitate which leads always to softening.

In the precipitation sequence in the Al–Au system, as the suggested [12] metastable precipitate defined as η' was proved [1,17] to be actually the incoherent equilibrium η precipitate which leads to softening during its early stages of growth, the softening behaviour is expected to dominate over the test temperature range above 523 K where the formation of η' precipitates (the stable η phase) take place. This is clear from the relaxation behaviour of the strength parameters σ_y, σ_f (Figs. 2a and b) and χ (Fig. 3) in their temperature dependence. This behaviour is also supported by the increase of both fracture strain ϵ_f (Fig. 2c) and dislocation slip distance L (Fig. 3). Besides, the coarsening of the precipitate will lead to an increased average inter-particle spacing, which causes a decrease of hardness, since the particles will be less effective in holding up dislocations.

The dependence of the coefficient of the work hardening on the deformation temperature (Fig. 3) might be interpreted as follows: The work hardening coefficient, χ, was calculated according to Mott's model [8]. This model attributes the work hardening to the activation of Frank-Read dislocation sources and the subsequent formation of pile-ups against obstacles such as grain boundaries. As the yield stress, and consequently the flow stress, decreased with increasing temperature (Fig. 2), the dislocation density in cell walls decreased [18]. Accordingly, the values of χ, which depend ultimately on dislocation density, decreased with increasing temperature. At any deformation temperature, increasing stress increases work hardening up to a certain critical stress σ_c, depending on the deformation temperature, above which softening behaviour takes place, as is obvious from Figs. 4a and b.

Plastic deformation of a polycrystalline metal or alloy is never uniform. Upon application of an external load, a process of deformation other than slipping [19], known as twinning, may take place in such metals as Au, Ag, Ni and many annealed fcc metals and alloys. The act of twinning takes place so suddenly to change the metal to such a state that the applied stress can produce slip. Accordingly, the softening observed above σ_c in Fig. 4 may be accounted for by the beginning of mechanical twin formation [20] at σ_c.

Indium addition caused general increase for all measured-strength parameters. It is known [21] that indium atoms have low solubility in Al and it is often observed that atoms with low solubility limits have a stronger tendency to segregate on grain boundaries [22] and on dislocations [23]. This is supported by the small average grain diameter (≈ 0.064 mm) measured using Fig. 7 for the ternary alloy samples, compared with that of the indium free samples (≈ 0.12 mm) done under the same conditions. Thus, during the quench and due to binding [24] between vacancies and both indium and gold atoms, vacancy–impurity clusters, which are thermally activated by 0.8 eV (see Fig. 5b and Table 1), are likely to be formed. It is possible that the addition of indium has a large effect on the distribution of vacancy clusters and modifying the structure of η precipitate by eliminating the coarse planar features and nonuniformities within the microstructure [25], so that

the activation energy for nucleation is reduced. The existing dislocations enhance [26] the nucleation rate of the coherent η precipitate. Therefore, it is expected that the finer and denser dispersion of the formed η precipitates leads to stronger pinning effect and consequently higher levels of hardening for all measured parameters of the samples containing indium. Besides, the quenched samples with indium still have higher strength level than the slowly-cooled samples. This might be due to the existing In-vacancy binding energy [24] which increases the heterogeneous nucleation of dislocation loops [27] which act as precipitation sites for η precipitates.

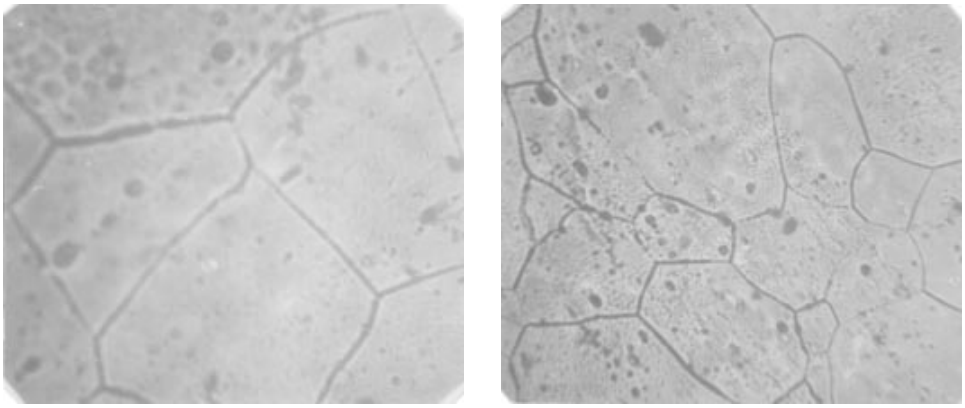

(a) G.D. = 0.12 mm (b) G.D. = 0.064 mm

Fig. 7. Photomicrographs showing grain size (G.D.) in (a) Al–*0.21wt%*Au *(250×), average G.D.= 0.12* mm*, (b)* Al–*0.21wt%*Au–*0.21wt%*In *(250×), average G.D.= 0.064* mm*. Samples of alloys* A *and* B *were solid solution treated at 793* K *for 4* h.

The high activation energy values given in Table 1 might be those that are required to activate mechanical twin formation, which involves change in orientation of one part of a crystal to a position symmetrical to the first part in slip. The increased number of the formed twins and the hardening effect due to indium addition may account for the increased energies at higher temperatures under stresses above the critical stress σ_c.

The general increase in the activation energy values, calculated in view of the strain hardening behaviour of the second stage and given in Table 1, might be required to: 1) activate the loss of coherence of η precipitates with the matrix above 523 K which leads to the variation of dislocation structures at the various stages of loss of coherency [1,14], 2) the dissolution of the small particles and the migration of the dispersed precipitate atoms across the increased separation of the large precipitates.

The microstructure variations shown in Fig. 6 might be due to the relief of the internal strains or stresses during the thermally activated growth of the stable incoherent η precipitates. This brings the matrix to a less deformed state. The

slowly-cooled samples showed marked variations over those of the quenched samples. This might be rendered (related) to the effect of the higher concentration of the quenched-in vacancies, which raise the internal strains and the lattice parameter of the quenched samples over those of the slowly-cooled ones.

5. *Conclusion*

Tensional testing at different temperatures of Al–0.21wt%Au and Al–0.21wt%Au –0.21wt%In alloys showed two stages or "double-m" strain hardening behaviour around 523 K. The critical stress σ_c characterizing the start of the second stage, i.e. the start of the parabolic part of the stress–strain curve, shifted towards lower stresses when increasing the deformation temperature.

The softening behaviour observed above the critical stress σ_c is due to a mechanical twin formation and/or loss of η precipitate coherency with the matrix. Solute atoms (Au and/or In)–vacancy pairs increase the strength levels of the tested samples.

The microstructure variations observed in tensile testing at different temperatures result from the relief of the internal strains or stresses during the growth of the stable incoherent precipitates.

References

[1] R. A. Ayres, Metall. Trans. A **10** (1979) 849.

[2] C. T. Kuonetal and J.Koreen, Inst. Met. **16** (1978) 90.

[3] C. Chen and G. Judd, Metall. Trans. A **9** (1978) 533.

[4] M. Von Heimendahl, Z. Metallkde. **58** (1967) 230.

[5] R. Sankaran and C. Laird, Phil. Mag. **29** (1974) 179.

[6] R. Sankaran and C. Laird, Acta Met. **24** (1976) 517.

[7] M. M. El-Sayed, phys. stat. sol. (a) **141** (1994) K103.

[8] N. F. Mott, Trans. AIME **218** (1960) 6.

[9] M. M. El-Sayed, F. Abd El-Salam and R. Abd El-Haseeb, phys. stat. sol. (a) **147** (1995) 401.

[10] J. H. Hollomon, Trans. AIME **162** (1945) 268.

[11] M. Atkinson, Metal. Trans. A **15** (1984) 1185.

[12] A. M. Abd El-Khalek, M. Sc. Thesis, Ain Shams Univ., Cairo, Egypt (1991).

[13] R. Sankaran and C. Laird, Acta Met. **22** (1974) 957.

[14] M. Von Heimendahl, Scripta Met. **10** (1976) 505.

[15] A. Z. Mohemed, M. M. Mostafa, M. S. Sakr and A. A. El-Daly, phys. stat. sol. (a) **110** (1988) K13.

[16] R. S. Mishra, A. G. Paradkar and K. N. Rao, Acta Metall. Mater. **41** (7) (1993) 2243.

[17] R. Sankaran and C. Laird, Scripta Met. **10** (1976) 507.

[18] M. Doyama, J. Nuclear Materials **69–70** (1978) 350.

[19] M. McCormak, G. W. Kammlott, H. S. Chen and S. Jin, Appl. Phys. Lett. **65** (9) (1994) 1100.

[20] F. Abd El-Salam, Egypt. J. Phys. **9** (2) (1978) 105.

[21] A. Bhattacharyya, G. V. S. Sastry and V. V. Kutumbarao, J. Mat. Sci. **34** (1999) 587.

[22] O. Vohringer, Z. Metalk. **67** (1976) 518.

[23] M. Hanson, *Constitution of Binary Alloys*, McGraw-Hill, New York (1958).

[24] F. Yang and S. Brook, Scripta Materialia **39** (6) (1998) 771.

[25] K. Iwasaki, J. Phys. Soc. Japan **49** (1980) 271.

[26] R. G. Hoagland, A. F. Voter and S. M. Foiles, Scripta Materialia **39** (4/5) (1998) 589.

[27] T. L. Davis and J. P. Hirth, J. Appl. Phys. **37** (1966) 2112.

UČINAK TEMPERATURE I DODATKA INDIJA NA MEHANIČKA SVOJSTVA LEGURE Al–0.21wt%Au

Istraživali smo istezna svojstva legura Al–0.21wt%Au i Al–0.21wt%Au–0.21wt%In na temperaturama 493 K do 553 K. Koeficijent mehaničkog očvršćivanja, $\chi = \partial\sigma^2/\partial\epsilon$, granica elastičnosti, σ_y, i granica loma, σ_f, smanjuju se pri povišenim temperaturama istezanja (T) te pokazuju nagao porast na oko 523 K. Nasuprot tome, lomno istezanje, ϵ_f, i prosječna duljina klizanja dislokacija, L, povećali su se s povišenom temperaturom istezanja, a pokazuju i minimum na oko 523 K. Radi objašnjenja opaženih promjena u procesu očvršćivanja ispitivanih uzoraka odredili smo aktivacijsku energiju na temperaturama oko 523 K.